This is an open access article published under a Creative Commons Attribution (CC-BY) License, which permits unrestricted use, distribution and reproduction in any medium, provided the author and source are cited.

Journal of Medicinal Chemistry

Article

Cite This: J. Med. Chem. 2018, 61, 804−817

pubs.acs.org/jmc

Neutral Porphyrin Derivative Exerts Anticancer Activity by Targeting Cellular Topoisomerase I (Top1) and Promotes Apoptotic Cell Death without Stabilizing Top1-DNA Cleavage Complexes

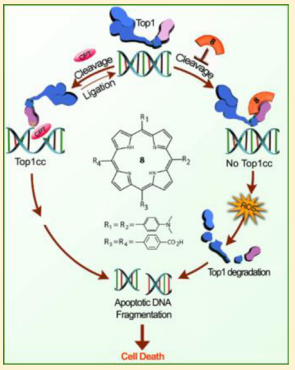
Subhendu K. Das,[†] Arijit Ghosh,[†] Srijita Paul Chowdhuri,[†] Nyancy Halder,[‡] Ishita Rehman,[†] Souvik Sengupta,[†,§] Krushna Chandra Sahoo,[‡] Harapriya Rath,*[,‡] and Benu Brata Das*[,†]

[†]Laboratory of Molecular Biology, Department of Biological Chemistry and [‡]Department of Inorganic Chemistry, Indian Association for the Cultivation of Science, 2A & 2B, Raja S. C. Mullick Road, Jadavpur, Kolkata 700032, India

[§]Division of Biological and Life Sciences, School of Arts and Sciences, Ahmedabad University, Central Campus, Navrangpura, Ahmedabad, Gujarat 380009, India

Supporting Information

ABSTRACT: Camptothecin (CPT) selectively traps topoisomerase 1-DNA cleavable complexes (Top1cc) to promote anticancer activity. Here, we report the design and synthesis of a new class of neutral porphyrin derivative 5,10-bis(4-carboxyphenyl)-15, 20-bis(4-dimethylaminophenyl)-porphyrin (compound **8**) as a potent catalytic inhibitor of human Top1. In contrast to CPT, compound **8** reversibly binds with the free enzyme and inhibits the formation of Top1cc and promotes reversal of the preformed Top1cc with CPT. Compound **8** induced inhibition of Top1cc formation in live cells was substantiated by fluorescence recovery after photobleaching (FRAP) assays. We established that MCF7 cells treated with compound **8** trigger proteasome-mediated Top1 degradation, accumulate higher levels of reactive oxygen species (ROS), PARP1 cleavage, oxidative DNA fragmentation, and stimulate apoptotic cell death without stabilizing apoptotic Top1-DNA cleavage complexes. Finally, compound **8** shows anticancer activity by targeting cellular Top1 and preventing the enzyme from directly participating in the apoptotic process.



INTRODUCTION

DNA topoisomerase I (Top1) is often exploited as an imperative anticancer chemotherapeutic target due to its critical role in DNA supercoil relaxation which involves three main steps: (a) DNA strand cleavage by a transesterification reaction initiated by the active site tyrosine attacking DNA phosphodiester backbone and generating a covalent intermediate of DNA 3′-phosphotyrosyl linkage (Top1cc), (b) DNA relaxation by controlled strand rotation, and (c) DNA religation by a similar transesterification and release of the enzyme from the DNA.[1−5]

Top1 inhibitors are classified into two groups, class I (poisons) and class II (catalytic inhibitors). Top1 poisons include camptothecin (CPT), topotecan, irinotecan, and other CPT derivatives as well as few non-CPT Top1 inhibitors like indenoisoquinolines, indolocarbazoles, and thiohydantoin derivatives that reveal their anticancer activity by selectively trapping the Top1-DNA covalent cleavage complexes (Top1cc) and inhibiting further religation of cleaved DNA strands.[2,3,6−8] Unrepaired Top1cc generates DNA double strand breaks following collision with replication or transcription machinery, which activates cell-cycle arrest and cell death.[3,9] In contrast, class II catalytic inhibitors hinder other steps of Top1 catalytic cycle by directly binding with enzyme but do not stabilize Top1cc which includes indolizinoquinolinedione.[10−14] All types of topoisomerase inhibitors cause DNA breaks and are accountable for the killing of the proliferating cancer cells.[3−5,9]

Drug independent trapping of Top1cc's are also evidenced from endogenous DNA lesions, like UV- and IR-radiation-induced DNA damage, abasic sites, oxidized bases, and mismatches.[3,9] Production of "apoptotic Top1cc" is independent of Top1 poisons but is dependent on variety of agents that are inducers of apoptotic cell death, including staurosporine, a protein kinase C inhibitor,[15] Top2 inhibitor like etoposide, and tubulin inhibitor like vinblastine.[16] All these compounds trigger cellular reactive oxygen species (ROS) that account for oxidative DNA damages that promote stabilization of Top1cc.[15,17,18]

Despite clinical success of CPT, the major limitations include its unstable chemical structure, poor aqueous solubility, and rapid cellular efflux via membrane pumps, and acquisition of cellular resistance of these drugs impelled the designing and investigation of new noncamptothecin Top1 inhibitors.[3,4] Porphyrins are a remarkably promising chemotype for development of anticancer agents and photodynamic therapy, which include FDA-approved and clinically used sensitizer Photofrin.[19,20] Porphyrin derivatives have wide pharmaceutical properties and broad range of biological activities that

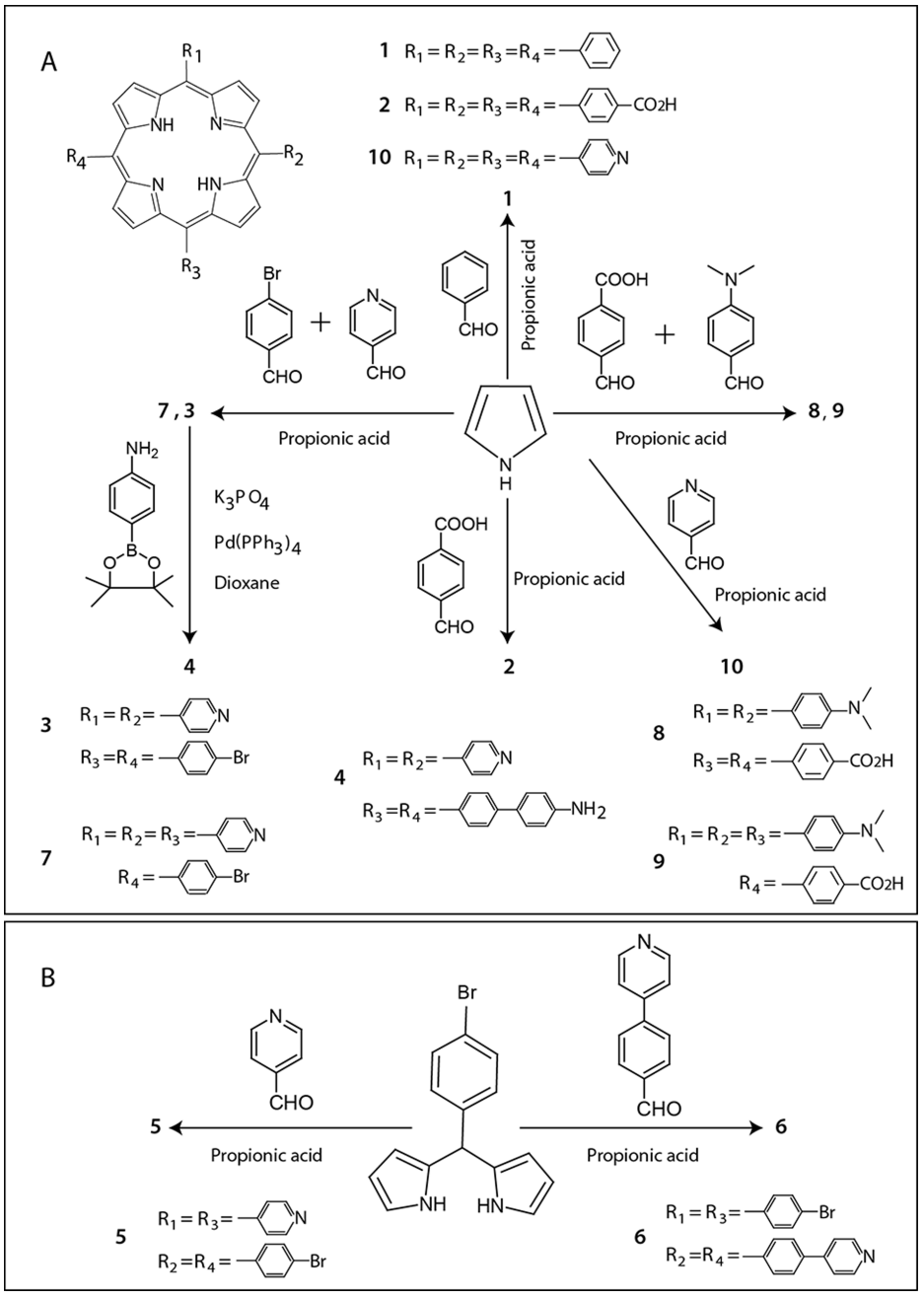
Received: September 6, 2017
Published: December 30, 2017

Downloaded via AHMEDABAD UNIV on May 1, 2025 at 10:41:11 (UTC).
See https://pubs.acs.org/sharingguidelines for options on how to legitimately share published articles.

© 2017 American Chemical Society

DOI: 10.1021/acs.jmedchem.7b01297
J. Med. Chem. 2018, 61, 804−817

Scheme 1. Synthesis of Library of Neutral Porphyrin Compounds



constitute selective modes of DNA binding, mimicking photosynthetic centers, vitamin B12, and P-450;[19,21−24] nevertheless, the cellular target of the compounds is still unclear.

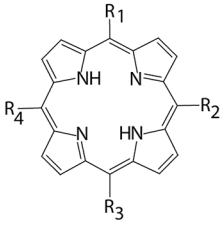
Here, we discuss our study involving design, synthesis, and biological evaluation of a novel series of neutral porphyrin that inhibits human Top1. Selected neutral porphyrin derivative 5,10-bis(4-carboxyphenyl)-15,20-bis(4-dimethylaminophenyl)-porphyrin (compound **8**) exhibited highest potency against human Top1 activity both as purified enzyme and as an endogenous protein in the total cellular extracts of human breast adenocarcinoma (MCF7) cells from our synthetic library. We have further established that the compound **8** binds with the free enzyme and targets cellular Top1 for proteasome-mediated degradation and bolsters ROS-induced apoptotic cell death without stabilizing Top1-DNA cleavage complexes. Persistent with inhibition of human Top1 activity in vitro, compound **8** was effective in killing cancer cells by targeting cellular Top1.

■ CHEMISTRY

The macrocycles under biological investigation described in our present manuscript are shown schematically (Scheme 1). We have taken into consideration the parent basic porphyrin, i.e., tetraphenylporphyrin, and variation in the periphery of the macrocycles with other *meso*-substituents. After investigating the biological properties of macrocycles compounds **1**, **2**, **3**, **4**, **5**, **6**, **7**, **9**, and **10**, we designed and synthesized **8** following the literature known synthetic methodology. Synthesis of porphyrins **1**,[25] **2**,[26] **3**,[27] **7**,[28] **8**, **9**, and **10**[29] were carried out following Adler method;[30] macrocycles bearing four identical *meso*-

DOI: 10.1021/acs.jmedchem.7b01297
J. Med. Chem. 2018, 61, 804−817

Table 1. Effective Drug Concentrations (EC_{50}) of Selected Neutral Porphyrin Compounds on the Recombinant Human Top1 (Top1) Plasmid DNA Relaxation Inhibition Assays

Core structure	Compound	Structure	Top1 inhibition EC_{50}(μM)	
			Simultaneous	Preincubation
	1	$R_1=R_2=R_3=R_4=$ 	>50	>50
	2	$R_1=R_2=R_3=R_4=$ 	2.015 ± 0.511	0.563 ± .19
	3	$R_1=R_2=$ $R_3=R_4=$	>50	>50
	4	$R_1=R_2=$ $R_3=R_4=$ 	82.78 ± 2.34	63.43 ± 1.89
	5	$R_1=R_3=$ $R_2=R_4=$	>50	>50
	6	$R_1=R_3=$  $R_2=R_4=$ 	>50	>50
	7	$R_1=R_2=R_3=$  $R_4=$ 	>50	>50
	8	$R_1=R_2=$  $R_3=R_4=$ 	**1.472 ± .32**	**0.381 ± .11**
	9	$R_1=R_2=R_3=$  $R_4=$ 	1.972 ± 0.411	1.226 ± .14
	10	$R_1=R_2=R_3=R_4=$ 	>50	>50

substituents such as compound **1**, **2**, and **10** were obtained by condensation of freshly distilled pyrrole and corresponding arylaldehyde under reflux condition using propionic acid as an acidic solvent. Furthermore, synthesis of compounds **3** and **8** (Scheme 1A) was tuned following the mixed-aldehyde condensation method leading to porphyrins bearing two different types of *meso*-substituents.[31] The A_3B type porphyrins **7** and **9** are often obtained in mixed-aldehyde condensation methods, and their yield was increased by reaction of 3:1 ratio of aldehydes A and B. It is a well-known fact that haloporphyrins undergo palladium-catalyzed cross-coupling reactions to produce alkyl-, vinyl-, aryl-, pyridyl-, and alkynylporphyrin monomers, dimers, and oligomers.[32] Thus, Suzuki coupling was carried out by strategically using a mixture of **3** and 4-aminophenylboronic acid pinacol ester to afford compound **4**[33] (Scheme 1A). Subsequently, the *trans*-substituted porphyrins, compounds **5**[34] and **6** (Scheme 1B), were synthesized based on the MacDonald 2 + 2 condensation of dipyrromethane (synthesized by acid-catalyzed condensation of pyrrole with 4-bromobenzaldehyde) with 4-pyridinecarboxaldehyde and 4-(pyridin-4-yl)benzaldehyde, respectively.[35] Detailed spectroscopic characterization data, elemental analysis results, and melting points of all the reported macrocycles in this manuscript have been documented in the Experimental Section and the Supporting Information (Figures S1−S40).

BIOLOGICAL RESULTS AND DISCUSSION

Neutral Porphyrin Derivative 8 Inhibits Human Topoisomerase 1 Catalytic Activity. To test the inhibitory effect of the synthetic library of neutral porphyrin compounds (Scheme 1) on human Top1 activity, we performed the DNA relaxation assays in a standard assay mixture containing the plasmid DNA and recombinant Top1.[6,13,36,37] Table 1 enlists the compounds with relative efficiencies of Top1 inhibition as a measure of their effective drug concentrations (EC_{50} value), indicating the highest activity for the selected neutral porphyrin derivative compound **8**.

To examine the mechanism of Top1 inhibition with compound **8**, we used variable incubation conditions in the relaxation assays (Figure 1A). When Top1 and compound **8** were mixed together in the relaxation assays (Figure 1A, lanes 13−16), 35−40% Top1 inhibition was achieved at 1 μM compound **8** (Figure 1A, lane 16). Next, to test the impact of compound **8** interaction with Top1 in the relaxation assays, we preincubated Top1 with compound **8** at indicated concentrations (Figure 1A, lanes 5−8) separately before the addition of DNA.[6,13,36,38] Under these conditions, 1 μM compound **8** was sufficient to induce 85−95% inhibition (Figure 1A, lane 8).

DOI: 10.1021/acs.jmedchem.7b01297
J. Med. Chem. 2018, 61, 804−817

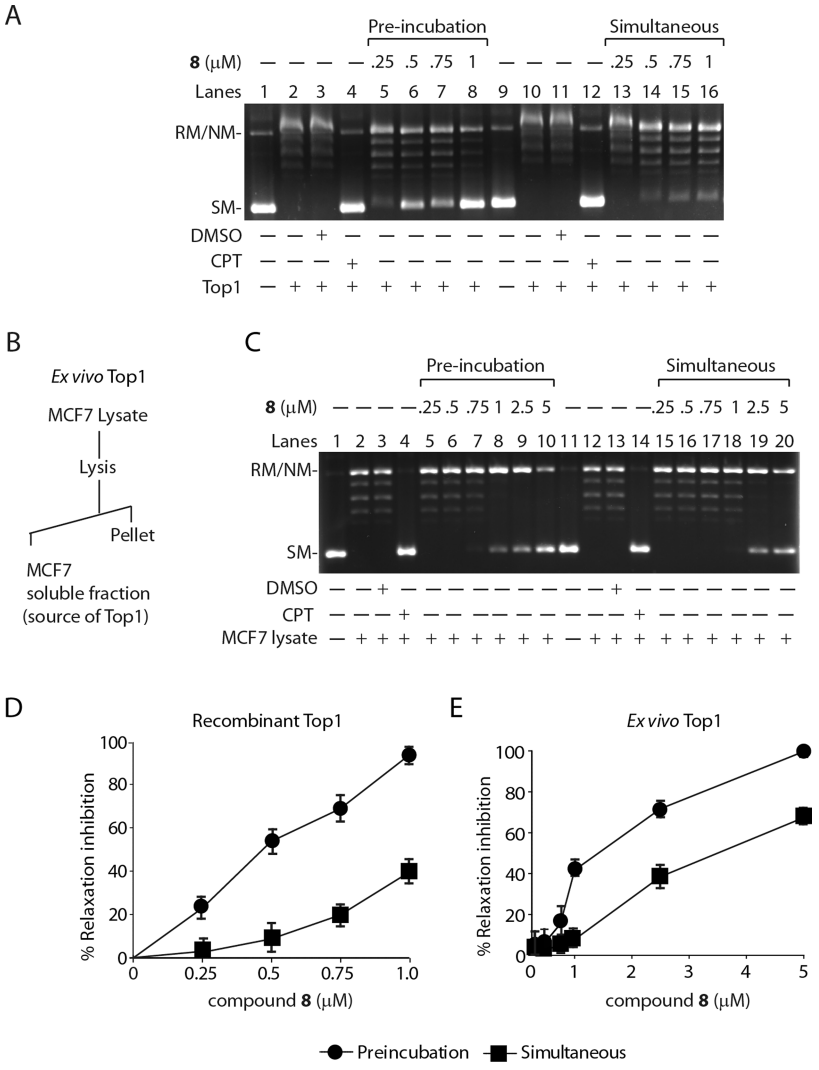


Figure 1. Compound **8** inhibits human Top1 catalytic activity both as recombinant enzyme and as an endogenous protein in the whole cell extracts of human breast adenocarcinoma (MCF7) cells. (A) Relaxation of supercoiled DNA with recombinant human Top1 at a molar ratio of 3:1. Lanes 1 and 9, pBS (SK^+) DNA (90 fmol); lanes 2 and 10, same as lane 1 but incubated with 30 fmol of Top1; lanes 3 and 11, same as lane 2 but Top1 was incubated with 2% DMSO; lane 4, same as lane 2 but Top1 preincubated with 2 μM CPT for 5 min; lanes 5−8, same as lane 2 but Top1 was preincubated with variable concentrations of compound **8** (as indicated) for 5 min followed by addition of DNA at 37 °C for 15 min; lane 12, same as lane 4 but CPT was incubated simultaneously with DNA and enzyme; lanes 13−16, same as lane 10 but simultaneously incubated with variable concentrations of compound **8** (as indicated) at 37 °C for 15 min. (B) Schematic representation for preparation of MCF7 whole cell lysates which was used as the source of endogenous Top1 for ex vivo Top1 relaxation assays. (C) Relaxation of supercoiled pBS (SK^+) DNA by Top1 activity from MCF7 cell extract (each reaction volume contains 0.1 μg protein). Lanes 1 and 11, pBS (SK^+) DNA (0.3 μg); lane 2 and 3, same as lane 1 but DNA was incubated with MCF7 cell lysates; lanes 3 and 13, same as lane 2 but incubated with 2% DMSO; lanes 4−10, same as lane 2 but MCF7 whole lysates were preincubated with 5 μM CPT or the variable concentrations of compound **8** (as indicated) for 5 min followed by addition of DNA at 37 °C for 15 min; lanes 14−20, same as lane 12 but MCF7 cell lysates were incubated simultaneously with 5 μM CPT or variable concentrations of compound **8** (as indicated) at 37 °C for 15 min. Positions of supercoiled monomer (SM) and relaxed and nicked monomer (RL/NM) are indicated. Quantitative representation for percentage relaxation inhibition (%) of recombinant Top1 (D) and endogenous Top1 (E) either preincubated or added simultaneously with Top1 with the variable concentrations of compound **8**. All the experiments were performed three times and expressed as the mean ± SD.

Panels A and D of Figure 1 show that Top1 inhibition was markedly increased (~4- to 5-fold) when compound **8** was preincubated with the recombinant enzyme compared to the simultaneous incubation (EC_{50} for Top1 inhibition preincubation: 0.381 ± 0.11 μM vs simultaneous 1.472 ± 0.32 μM), suggesting that compound **8** may bind to the free enzyme, unlike CPT to inhibit Top1 activity.

To investigate the selectivity of compound **8** toward endogenous Top1 in the whole cell extracts of human breast adenocarcinoma (MCF7) cells (Figure 1B), we used ex vivo Top1 relaxation inhibition assays.[6,39] The advantage of employing whole cell extracts as source of Top1 is that the enzyme is maintained in its native structure among a plethora of other proteins. Figure 1C shows that compound **8** markedly inhibited Top1 activity when the cellular extracts were preincubated with compound **8** (Figure 1C, lanes 5−10) compared to simultaneous incubation (Figure 1, panel C, lanes 15−20). Quantification indicates that Top1 inhibition was significantly increased (~2- to 3-fold) when compound **8** was preincubated with whole cell extracts (Figure 1E), consistent

DOI: 10.1021/acs.jmedchem.7b01297
J. Med. Chem. 2018, 61, 804−817

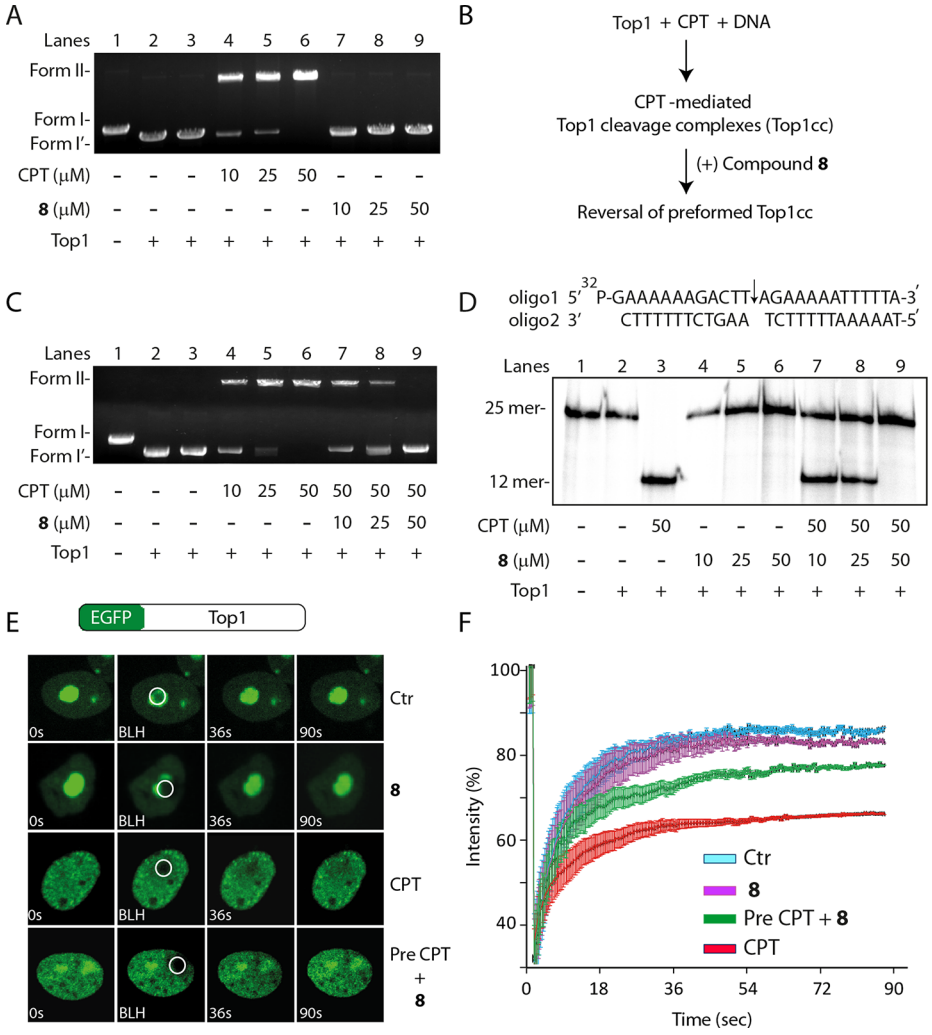


Figure 2. Compound **8** inhibits formation of Top1-DNA cleavage complexes and abrogates CPT-mediated DNA cleavage complex stabilization. (A) Representative gel showing Top1 mediated plasmid DNA cleavage in the presence of CPT or compound **8**. Lane 1, 50 fmol of pBS (SK^+) supercoiled DNA. Lanes 2−9, same as lane 1 but incubated with equal amounts of recombinant human Top1 (100 fmol) at the indicated concentrations of CPT or compound **8** or only DMSO at 37 °C for 30 min. Positions of supercoiled substrate (form I) and nicked monomers (form II) are indicated. (B) Experimental design to test the impact of compound **8** on CPT-mediated preformed Top1 cleavage complex (Top1cc). (C) Compound **8** abrogates CPT-mediated cleavage. Lane 1, 50 fmol of pBS (SK^+) supercoiled DNA. Lanes 2−6, same as lane 1 but incubated with equal amounts of Top1 (100 fmol) at the indicated concentrations of CPT or compound **8**. Lanes 7−9, same as lane 1 but incubated with equal amounts of Top1 with CPT before addition of compound **8** as indicated at 37 °C for 30 min. (D) Representative gel showing Top1-mediated 25 mer duplex oligonucleotide cleavage in the presence of CPT and compound **8**. Lane 1, 10 nM 5′-^{32}P-end labeled 25-mer duplex oligo as indicated above. Lane 2, same as lane 1 but incubated with recombinant Top1 (0.2 μM). Lanes 3−6, same as lane 2 but incubated with indicated concentration of CPT or compound **8**. Lanes 7−9, same as lane 2 but incubated with equal amounts of Top1 with CPT before addition of indicated concentrations of compound **8** at 37 °C for 30 min. Positions of uncleaved oligonucleotide (25-mer) and the cleavage product (12-mer oligonucleotide complexed with residual Top1) are indicated. (E) Compound **8** inhibits formation of Top1-DNA bound complexes (Top1cc) in live cells. Representative images showing the fluorescence recovery after photobleaching (FRAP) of enhanced green fluorescence tagged-human Top1 (EGFP-Top1) transiently expressed in MCF7 cells and their response to CPT (5 μM), compound **8** (20 μM) separately treated for 10 min or pretreatment with CPT (5 μM) for 10 min followed by treatment of compound **8** (20 μM) for 10 min (Pre CPT + **8**). A subnuclear spot (ROI) indicated by a circle was bleached (BLH) for 30 ms and photographed at regular intervals of 3 ms thereafter. Successive images taken for ∼90 s after bleaching illustrate fluorescence return into the bleached areas. (F) Quantification of FRAP data (n = 15) showing mean curves of Top1 in the presence of CPT or compound **8**. Error bars represent the standard error of the mean.

with the inhibition of recombinant Top1 in preincubation relaxation assays (Figure 1D).

Here we provide evidence that compound **8** selectively inhibits Top1, both as a purified enzyme (Figure 1A) and as an endogenous protein in the total cellular lysate (Figure 1C) without being afflicted by other proteins. Therefore, it is conceivable that compound **8** selectively interacts with human Top1 to promote the inhibition of DNA relaxation activity.

Compound 8 Inhibits Top1-DNA Cleavage Complexes. Because camptothecin (CPT) stabilizes Top1-DNA cleavable complexes (Top1cc) to inhibit Top1 activity,[3,5,37] we investigated compound **8** induced Top1cc formation with the plasmid DNA cleavage assays.[6,8,36,37] Top1 mediated conversion of closed circular DNA (form I) to nicked circular DNA (form II) in the presence of specific inhibitors is referred to as "cleavable complex". Figure 2A shows that compound **8** failed to stabilize Top1cc in contrast to CPT, suggesting that

DOI: 10.1021/acs.jmedchem.7b01297
J. Med. Chem. 2018, 61, 804−817

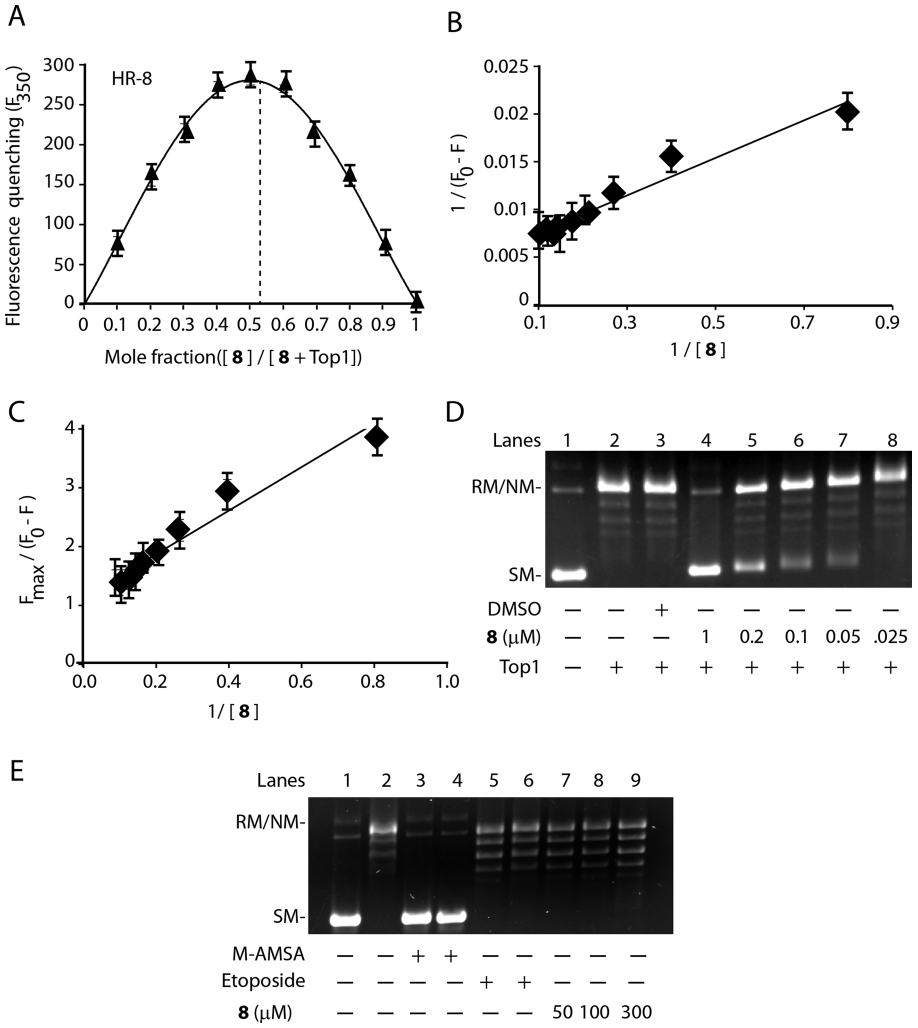


Figure 3. Compound **8** reversibly binds with Top1 at equimolar concentration. (A) Job's plot of compound **8** binding to Top1. Data are represented as the mean ± SD from three independent experiments. (B) Double reciprocal plot of inhibitor binding to Top1. Data are represented as the mean ± SD from three independent experiments. (C) Linear plot of binding of compound **8** to Top1. Data are represented as the mean ± SD from three independent experiments. (D) Compound **8** binds with Top1 in reversible manner. Lane 1, 50 fmol of pBS (SK^+) DNA. Lane 2, recombinant Top1 (100 fmol) was preincubated with the reaction mixture at 37 °C for 5 min before addition of pBS (SK^+) DNA. Lane 3, same as lane 2 but in the presence of 2% v/v DMSO. Lane 4, same as lane 2 but in the presence of 1 μM compound **8**, preincubated with Top1 for 5 min at 37 °C in relaxation buffer followed by addition of 50 fmol of pBS (SK^+) DNA and was further incubated for 15 min at 37 °C. Lane 5−8, same as lane 4 but diluted to 5-, 10-, 20-, and 40-fold so that the final inhibitor concentrations became 0.2, 0.1, 0.05, and 0.025 μM compound **8**. These were followed by addition of DNA and were further incubated for 15 min at 37 °C. The experiments were performed three times, and representative result is from one set of experiments. (E) Compound **8**−DNA interaction as studied by agarose gel electrophoresis. Lane 1, 50 fmol of pBS (SK^+) DNA. Lane 2, relaxed pBS (SK^+) DNA generated by excess of Top1. Lanes 3−6, same as lane 2 but incubated with 50 and 300 μM m-AMSA and etoposide, respectively. Lanes 7−9, same as lane 2 but incubated with 50, 100, 300 μM of compound **8** as indicated.

compound **8** inhibits Top1cc formation. To further investigate the impact of compound **8** on preformed Top1cc, we preincubated Top1 with plasmid DNA and CPT (Figure 2B) before the addition of compound **8** in the cleavage assays. Figure 2C shows that compound **8** completely abrogated CPT-induced Top1cc in a dose dependent manner (Figure 2, panel C, lanes 7−9).

In contrast to CPT (Figure 2D, lane 3), we further established that compound **8** failed to stabilize Top1cc in single turnover equilibrium cleavage assays (Figure 2D, lanes 4−6) by reacting recombinant Top1 with 25-mer duplex oligonucleotides harboring preferred Top1 cleavage sites.[1,13,36,38] In addition, compound **8** reversed the CPT-induced Top1cc with 12-mer cleaved oligonucleotides (Figure 2D, lane 7−9) consistent with plasmid DNA cleavage assays (Figure 2C). Taken together, our data indicate that compound **8** inhibits Top1 without trapping Top1cc.

To obtain direct evidence for compound **8** mediated inhibition of Top1cc formation in live human carcinoma cells, we used MCF7 cells and transiently expressed EGFP-Top1. Live cells expressing ectopic Top1 were analyzed under laser confocal microscopy equipped with fluorescence recovery after photobleaching (FRAP) technology.[40−42] The FRAP recovery curves of EGFP-Top1 in the untreated samples represent a large (∼80−85%) mobile population (see Figure 2E and Figure 2F; Ctr) compared to a small (∼20%) immobile population, suggesting that Top1 is dynamic, freely exchanged and binds transiently with the DNA (reversible Top1cc).[42]

However, CPT covalently trapped Top1 on the DNA in the live cells (Figure 2E; CPT), which significantly impedes FRAP

DOI: 10.1021/acs.jmedchem.7b01297
J. Med. Chem. 2018, 61, 804−817

recovery by increasing ~40−50% of Top1 immobile population (Figure 2E and Figure 2F; (+) CPT; 5 μM). Under similar conditions fluorescence recovery of EGFP-Top1 was unaffected in the presence of compound **8** (Figure 2E and the quantification in Figure 2F; (+) compound **8**; 20 μM), indicating compound **8** failed to trap Top1cc in live cells. Furthermore, compound **8** can restore ~12−15% of Top1 mobility in cells pretreated with CPT (Figure 2E,F), suggesting compound **8** promotes reversal of CPT-induced Top1cc in live cells consistent with the in vitro cleavage assays (Figure 2A−D). Taken together our data provide evidence that compound **8** inhibits cellular Top1cc formation.

Compound 8 Reversibly Binds with Top1 at Equimolar Concentration. Next we investigated the binding nature of compound **8** with the purified Top1 by measuring the intrinsic tryptophan fluorescence quenching of Top1. Figure 3A shows 1:1 binding stoichiometry of compound **8** with Top1 as measured from Job plot,[12,14,43] suggesting that there is one binding site for the drug in the enzyme. Figure 3B and Figure 3C shows the quenching profile of Top1 in the presence of variable doses of compound **8**, with a dissociation constant (K_D = 0.381 μM) calculated from Figure 3B and Figure 3C.

To further investigate the nature of binding of compound **8** with Top1 (reversible vs irreversible),[12,14] we performed dilution assay with recombinant Top1. Top1 was preincubated with 1 μM compound **8** at which 90−99% inhibition of enzyme has been achieved (Figure 3D, lane 4). The subsequent dilution of the reaction mixtures in the relaxation assays showed an increase in the % relief of inhibition for compound **8**. Complete relief of Top1 inhibition was achieved at 40-fold dilution (Figure 3D, lane 5−8). This suggests that compound **8** interacts in a reversible manner with Top1, consistent with its weak dissociation constant.

To investigate the intercalation capacity of the compound **8** into the plasmid DNA, we performed topoisomerase I unwinding assays,[36,44] which depend on the capacity of intercalating compounds to unwind the duplex DNA and thereby induce a conformational change in the DNA.[36,44] Figure 3E demonstrates that m-AMSA, a strong DNA intercalative agent, incites a net negative supercoiling of the relaxed plasmid DNA at concentration independent manner (Figure 3E, lanes 3 and 4). Under similar conditions nonintercalative compounds like etoposide failed to show such effect (Figure 3E, lanes 5 and 6). Figure 3E, lanes 7, 8, 9, shows that compound **8** failed to induce negative supercoiling of the relaxed plasmid DNA at 50, 100, 300 μM concentrations, suggesting neutral porphyrin derivative **8** is not a DNA intercalator. Therefore, compound **8** interacts in reversible manner with Top1 to inhibit the plasmid relaxation activity (Figure 1).

Compound 8 Triggers Proteasome-Mediated Degradation of Cellular Top1 without Stabilizing Apoptotic Top1-DNA Covalent Complexes. Because compound **8** binds with free Top1 (Figure 3) and inhibits Top1cc formation in live cells (Figure 2E), we examined the impact of compound **8** on endogenous Top1. Cellular lysates were prepared from MCF7 cells treated with compound **8** for indicated times and were analyzed by Western blotting. Figure 4A, lanes 2−4, shows time dependent depletion of Top1 signal in compound **8** treated cells, suggesting Top1 degradation. Because proteasome has been implicated for Top1 degradation,[7,9,45] we used proteasome specific inhibitor (MG132) to investigate Top1 proteolysis in compound **8** treated cells. Figure 4B confirmed

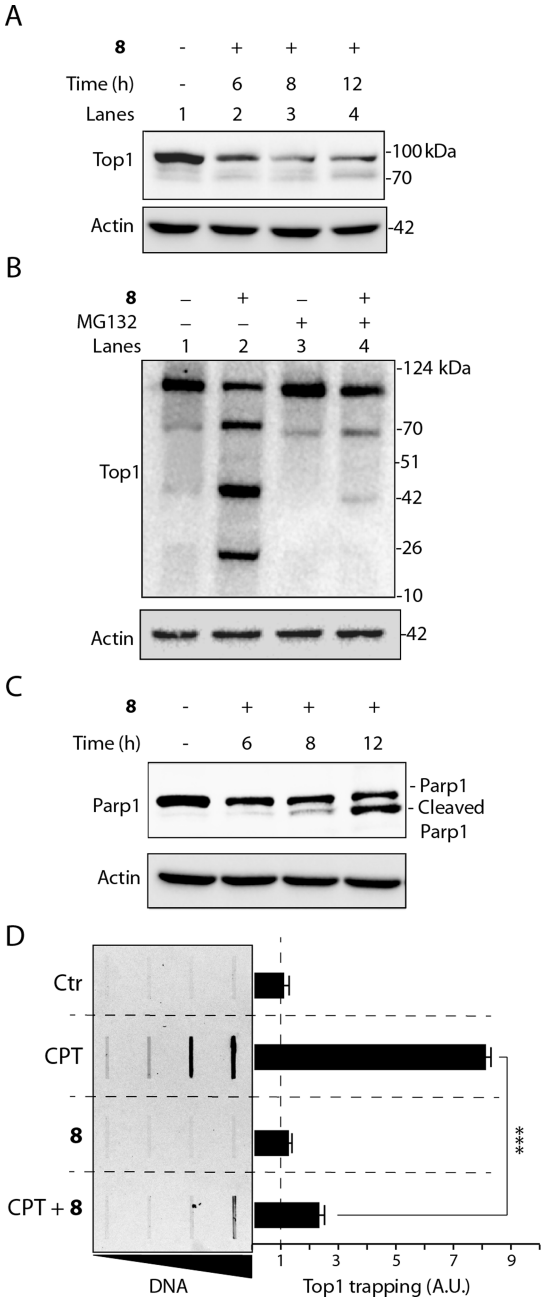


Figure 4. Compound **8** induces proteasome-mediated degradation of cellular Top1 and apoptotic PARP1 cleavage without stabilizing apoptotic Top1-DNA covalent complexes. (A) Western blot analysis of Top1 in whole cell extracts of MCF7 cells treated with compound **8** (10 μM) for indicated time. (B) Western blot analysis of Top1 in whole cell extracts from MCF7 cells without treatment (lane 1) or treated with compound **8** (10 μM) (lane 2) or MG132 (100 nM; proteasome inhibitor) (lane 3) or preincubated with MG132 for 4 h followed by addition of compound **8** for 12 h. Numbers are molecular masses in kDa. (C) Western blot analysis of PARP1 in whole cell extracts from MCF7 cells treated with compound **8** (10 μM) for indicated times. Positions of PARP1 full length and cleaved PARP1 are indicated. (D) Detection of Top1cc by ICE bioassays in MCF7 cells treated with CPT (10 μM) or compound **8** (20 μM) for 12 h or pretreated with CPT for 6 h before the addition of compound **8** was further incubated for 6 h. Genomic DNA at increasing concentrations (0.5, 1, 2, 4 μg) was probed with an anti-Top1 antibody. The bar represents quantification of Top1cc (n = 3; calculated value ± SEM) under different drug treatment. Asterisks denote significant difference ((***) $P < 0.001$; t test).

DOI: 10.1021/acs.jmedchem.7b01297
J. Med. Chem. 2018, 61, 804−817

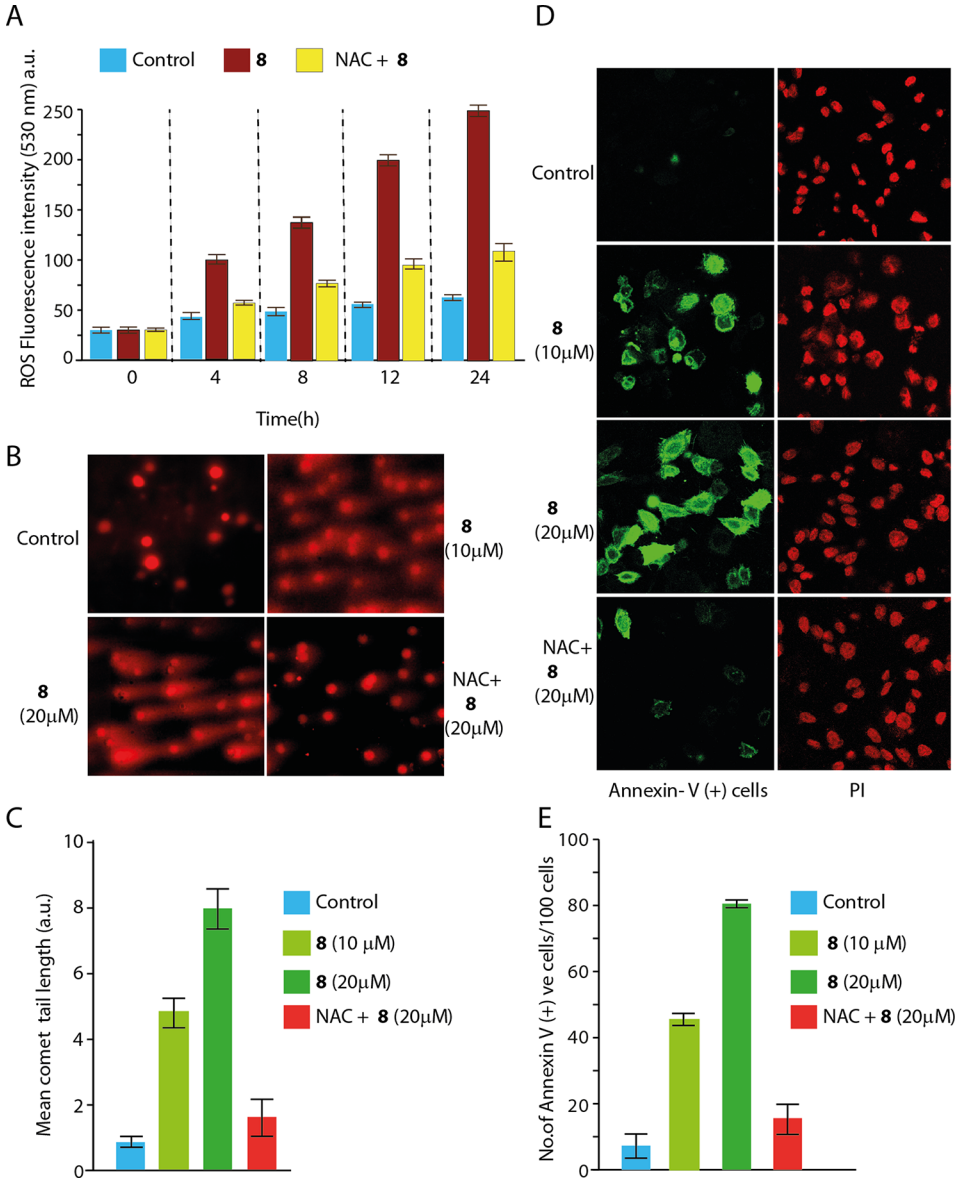


Figure 5. Compound **8** activates reactive oxygen species (ROS) induced oxidative DNA breaks and promotes apoptotic cell death. (A) Generation of ROS was measured using the fluorescent dye CM-H2DCFDA in MCF7 cells after treatment with 0.2% DMSO alone (blue bar) or with 10 μM compound **8** (red bar), and pretreatment with *N*-acetylcysteine (NAC; 10 mM) for 30 min prior to treatment with compound **8** (yellow bar) for indicated times. Data are expressed as mean ± SD of three independent experiments. (B) Representative images of alkaline comet assays with MCF7 cells treated with compound **8** for 12 h or pretreatment with NAC (10 mM) for 30 min prior to treatment with compound **8** as indicated. (C) Quantification of drug induced mean comet tails were calculated for 20−25 cells (average ± SEM). (D) Representative confocal microscopy images showing apoptosis marker phosphatidylserine as detected with annexin V-FITC antibody (green) after compound **8** treatment for 12 h or pretreatment with NAC (10 mM) for 30 min prior to compound **8** as indicated. Cells were counterstained with propidium iodide (PI; red) to visualize nuclei. (E) Quantification of drug induced annexin V (+) cells were calculated from ∼100 cells (average ± SEM) as indicated.

that **8**-induced degradation of Top1 (Figure 4B, lane 2) was abrogated in the presence of proteasome inhibitor MG132 (Figure 4B, lane 4), suggesting compound **8** activates proteasome pathway.

Next, to investigate the plausibility between Top1 proteolysis and activation of apoptosis, we tested PARP cleavage, a "hallmark" event of apoptosis in compound **8** treated cells.[16−18,46,47] Figure 4C shows that compound **8** treatment for 12 h indeed promotes PARP cleavage, suggesting compound **8** activates apoptosis through degradation of Top1.

Because compound **8** stimulates apoptosis (Figure 4C and Figure 5B), we examined accumulation of apoptotic Top1-DNA complexes in compound **8** treated cells (Figure 4D) by ICE bioassays.[15,16] Top1cc related to apoptosis is due to secondary DNA modifications and is independent from direct Top1-drug interaction.[15−17] Under a condition that triggers PARP1 cleavage in MCF7 cells treated with compound **8**, immunoblotting revealed the absence of Top1 in the DNA-containing fractions (Figure 4D; compound **8**), in contrast to camptothecin (Figure 4D; CPT), indicating that compound **8** inhibits Top1cc during apoptosis. Compound **8** abrogates CPT-induced cellular Top1-DNA complexes (Figure 4D; CPT + **8**), in keeping with in vitro cleavage assays (Figure 2B). Therefore, proteasome mediated degradation of Top1 triggers compound **8** induced apoptosis without stabilizing apoptotic Top1-DNA covalent complexes.

DOI: 10.1021/acs.jmedchem.7b01297
J. Med. Chem. 2018, 61, 804−817

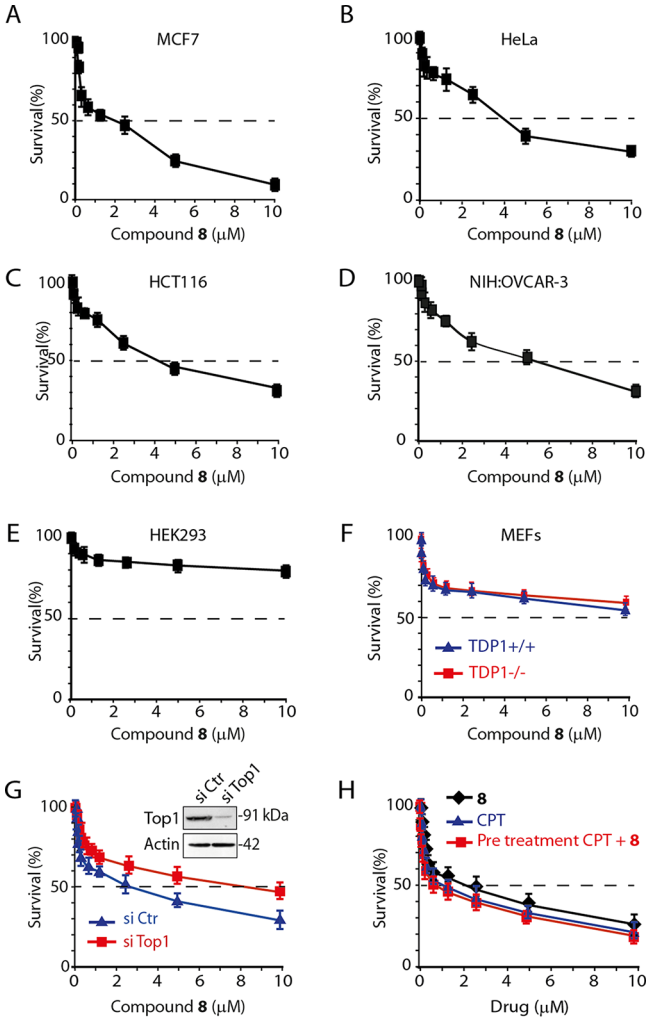
Compound 8 Accumulates Reactive Oxygen Species Induced DNA Breaks and Promotes Apoptotic Cell Death. Next, to investigate the mechanistic link between compound **8** induced cellular Top1 inhibition (Figure 1), degradation (Figure 4A and Figure 4B), and activation of apoptosis (Figure 4C), we tested reactive oxygen species (ROS) formation and accumulation of oxidative DNA fragmentation[15,17,46] in compound **8** treated MCF7 cells. To examine ROS accumulation, we used nonfluorescent substrate (2′,7′-dichlorodihydrofluorescein diacetate; H2DCFDA) which is transformed into fluorescent product (2′,7′-dichlorofluorescein; DCF) in the presence of ROS inside the cells.[13] Figure 5A shows time dependent accumulation of ROS in compound **8** treated cells. We observed a marked elevation (~3- to 5-fold) in ROS accumulation (Figure 5A) under similar conditions that activate PARP1 cleavage (Figure 4C). Nonetheless, MCF7 cells pretreated with *N*-acetylcysteine (NAC), a specific inhibitor of ROS, reduced compound **8** induced ROS generation by ~3-fold (Figure 5A).

One interpretation of this result is that compound **8** induced ROS may accumulate oxidative DNA strand breaks that activate apoptosis[3,13] as revealed by PARP1 cleavage (Figure 4C). Therefore, we directly measured compound **8** induced DNA strand breaks at single cellular level by using alkaline comet assays (Figure 5B,C) and simultaneously measured the apoptotic cell death by immunofluorescence staining of the apoptosis marker phosphatidylserine with annexin V-FITC antibody (Figure 5D,E). Compound **8** treated MCF7 cells accumulate ~8-fold increase in DNA strand breaks (Figure 5B and Figure 5C) compared to untreated cells, resulting in ~7-fold elevation in compound **8** induced annexin V(+) apoptotic cells (Figure 5D and Figure 5E). We further confirmed that ROS inhibitor NAC resulted in ~4-fold decrease in compound **8** induced DNA breaks (Figure 5C) as well as ~4- to 5-fold reduction in annexin V(+) apoptotic cells (Figure 5E). Therefore, we conclude that compound **8** triggers reactive oxygen species induced DNA degradation and apoptotic cell death without stabilizing Top1-DNA cleavage complexes.

Compound 8 Displays Potent Anticancer Activity. Compound **8** was investigated for its cytotoxicity in the cancer cell lines from different tissue origin,[6,41] as well as in the noncancerous human embryonic kidney cell lines (HEK293) and mouse embryonic fibroblasts (MEFs). Figure 6 indicates that compound **8** revealed potent cytotoxicity in cancerous cells including human breast adenocarcinoma cell lines (MCF7, IC_{50} = 2.17 μM), human cervical cancer cell lines (HeLa, IC_{50} = 4.13 μM), human ovarian adenocarcinoma cell lines (NIH:OVCAR-3, IC_{50} = 5.19 μM), and human colon carcinoma cell lines (HCT116, IC_{50} = 4.39 μM) cells, compared to the non cancerous cells like HEK293 or MEFs that show markedly reduced or no toxicity (IC_{50} > 10 μM). The MCF7 breast cancer cell lines were most susceptible to compound **8**.

TDP1 hydrolyzes 3′ phosphotyrosyl linkages that are primarily due to Top1cc; therefore TDP1−/− cells are hypersensitive to Top1 poisons.[40,41,45,48] Figure 6F shows that both TDP−/− and TDP1+/+ MEFs cells were equally sensitive to compound **8**, further providing evidence that compound **8** exerts cytotoxicity without stabilizing Top1cc (Figure 4D).

To further confirm that Top1 is the cellular target for compound **8** mediated cytotoxicity, we have performed cytotoxicity assays in siRNA mediated Top1 knockdown cells (Figure 6G, inset). Figure 6G indicate that compound **8** treated Top1 knockdown cells displayed reduced cytotoxicity compared to the Top1 proficient cells, establishing that Top1 is the cellular target for compound **8**.



I

Cell lines	IC_{50}(μM)	Cell lines	IC_{50}(μM)
MCF7	2.17 ± 0.06	HeLa	4.13 ± 0.05
HCT116	4.39 ± 0.08	NIH:OVCAR-3	5.19 ± 0.07
HEK293	> 10	TDP1+/+	> 10
SiRNA Ctr	2.24 ± 0.09	TDP1-/-	> 10
SiRNA Top1	8.15 ± 0.06		

Figure 6. Compound **8** shows potent anticancer activity mediated through topoisomerase 1. The graphical representation of percentage survival (%) of (A) MCF7, (B) HeLa, (C) HCT116, (D) NIH:OVCAR-3, (E) HEK293, (F) MEFs (TDP+/+ and TDP−/−) cells was plotted as a function of indicated compound **8** concentrations. (G) Top1 knockdown cells are less sensitive to compound **8**. Following transfection with Top1 or control (Ctr) siRNA for 72 h, MCF7 cells were analyzed by Western blotting to confirm Top1 knockdown. Actin served as loading control (inset). Percentage survival (%) of MCF7 cells transfected with Top1 or Ctr siRNA was plotted as a function of indicated compound **8** concentrations. (H) Graphical representation of percentage survival (%) of MCF7 cells treated with compound **8** or CPT separately or cells were pretreated with CPT (5 μM) for 12 h prior to addition of compound **8** as indicated. The percent inhibition of viability for each concentration of compound **8** was calculated with respect to the control, and IC_{50} (μM) values were estimated. Each point corresponds to the mean ± SD of at least three experiments in duplicates. Error bars represent SD (n = 3).

DOI: 10.1021/acs.jmedchem.7b01297
J. Med. Chem. 2018, 61, 804−817

Because compound **8** exerts cytotoxicity without stabilizing Top1cc (Figure 4D), next we tested the impact of compound **8** on CPT-induced preformed Top1cc. Figure 6H shows that pretreatment of CPT and further addition of compound **8** were not additive in cytotoxicity but showed overlapping cytotoxicity in MCF7 cells treated with compound **8** or CPT independently. Therefore, we conclude compound **8** plausibly suppresses the CPT induced cytotoxicity (Figure 6H) because compound **8** reverses CPT-induced Top1cc formation in cells as well as in cleavage assays (Figure 2). Taken together these data suggest that compound **8** is a potential Top1 inhibitor and may be an appropriate lead to develop as a potential anticancer agent.

CONCLUSION

In summary, we have identified neutral porphyrin based compound **8** as a new potent anticancer agent that inhibits cellular Top1 without trapping Top1-DNA cleavage complexes, a mechanism that is unique in comparison to known Top1 poisons like camptothecin (CPT). We provide evidence that in contrast to CPT, the selected porphyrin derivative **8** binds reversibly to the free enzyme (Figure 3) and effectively inhibits the formation of Top1-DNA cleavage complex (Top1cc) both in vitro and in live cell as determined in FRAP assays (Figure 2). Compound **8** abrogates CPT-mediated preformed Top1cc both as recombinant enzyme (Figure 2A-D) and as an endogenous Top1 in the human breast adenocarcinoma (MCF7) cells (Figure 4D), suggesting a plausibility to overcome the limitations of CPT resistance.

ROS-induced DNA damage facilitates trapping of Top1cc in cells and is an obligatory event in the progression of apoptosis.[15−17] In contrast, compound **8** activates reactive oxygen species (ROS), proteolysis of cellular Top1, which may accumulate DNA torsional strain resulting oxidative DNA damage as revealed by alkaline comet assays and apoptotic cell death (Figure 5) without stabilization of apoptotic Top1-DNA complexes (Figure 4D). Therefore, compound **8** counteracts the cellular Top1 by abrogating its precise engagement in the apoptotic process.

We further show that in contrast to noncancerous cells, compound **8** is effective against cancerous cell lines from different tissue origin including MCF-7, HeLa, NIH:OVCAR-3, and HCT116 cells (Figure 6) by targeting cellular Top1 (Figure 6G). A future challenge includes development of more potent neutral porphyrin based Top1 catalytic inhibitor, which may be exploited for anticancer therapy.

EXPERIMENTAL SECTION

Chemistry. General Methods. Electronic absorption spectra were measured with a PerkinElmer Lambda 950 UV−visible−NIR spectrophotometer. ^{1}H NMR spectra were recorded on a Bruker AVIII 500 MHz spectrometer, and chemical shifts were reported as the δ scale in ppm relative to $CHCl_3$ (δ = 7.26 ppm) and DMSO (δ = 2.50 ppm) as internal reference for ^{1}H. MALDI-TOF MS data were recorded using Bruker Daltonics flex analyzer. All solvents and chemicals were of reagent grade quality, obtained commercially and used without further purification except as noted. For spectral measurements, anhydrous dichloromethane was obtained by refluxing and distillation over CaH_2. Gravity column chromatography was performed using Merck silica gel 230−400 mesh. All reported yields refer to pure isolated compounds. Chemicals and solvents were of reagent grade and used as obtained from commercial sources without further purification. The purities of all of the biologically tested compounds were the peak area of the major product, being ≥95% as estimated by NMR spectroscopy and C, H, N analysis along with melting point.

Synthesis. 5,10,15,20-Tetraphenylporphyrin (1). By use of a general method, 1 mL (10 mmol) of benzaldehyde and 50 mL of propionic acid were mixed and the reaction mixture was magnetically stirred. Freshly distilled pyrrole (0.7 mL; 10 mmol) was then added to the mixture, and the temperature was then brought to reflux and allowed to stir for 2 h at reflux. After allowing the reaction mixture to cool to room temperature, the reaction flask was placed in the freezer overnight to aid precipitation of the porphyrin. The reaction mixture was then vacuum filtered using a sintered funnel, and a dark purple solid was collected, washed with 5 × 50 mL of DCM, washed with methanol, dried overnight, and purified by silica gel chromatography to give 4.9 g, of 5,10,15,20-tetraphenylporphyrin (79% yields). Mp > 300 °C. ^{1}H NMR (500 MHz, $CDCl_3$ 298 K, δ [ppm]) 8.88 (s, 8H, py), 8.25 (m, 8H, Ph-CH), 7.79 (m, 12H, Ph-CH), −2.76 (s, 2H, -NH). UV−vis (CH_2Cl_2, λ [nm], 298 K): 417 nm, 515 nm, 548 nm, 590 nm, 645 nm. MALDI-TOF MS (m/z): 615.635 (calcd for $C_{44}H_{30}N_4$ exact mass, 614.206). Anal. Calcd for $C_{44}H_{30}N_4$: C, 85.97; H, 4.92; N, 9.11. Found: C, 86; H, 5.00; N, 9.08.

5,10,15,20-Tetrakis(4-carboxyphenyl)porphyrin (2). By use of a general method, 1.5 g (10 mmol) of 4-formylbenzoic acid and 50 mL of propionic acid were added, and the reaction mixture was stirred at ambient temperature. To increase the solubility of 4-formylbenzoic acid, the reaction mixture was heated to 80 °C at which point the aldehyde fully dissolved. Freshly distilled pyrrole (0.7 mL; 10 mmol) was then added to the mixture, and reaction mixture was allowed to stir for 2 h under reflux. The reaction mixture was cooled to room temperature and placed in the freezer overnight to aid precipitation of the porphyrin. The reaction mixture was then vacuum filtered using a sintered funnel and a dark purple solid was collected, washed with 5 × 50 mL of DCM, washed with methanol, and dried overnight to give 1.1 g, of 5,10,15,20-tetrakis (4-carboxyphenyl)porphyrin (55% yields). Mp > 300 °C. ^{1}H NMR (500 MHz, DMSO-d_6 298 K, δ [ppm]) 13.14 (4H, br, -COOH), 8.86 (8H, s, Py β-H), 8.38 (16H, dd, phenyl H), −2.93 (2H, s, NH). UV−vis (CH_3OH, λ [nm], 298 K): 413 nm, 513 nm, 545 nm, 589 nm, 646 nm. MALDI-TOF MS (m/z): 790.604 (calcd for $C_{48}H_{30}N_4O_8$ exact mass, 790.206). Anal. Calcd for $C_{48}H_{30}N_4O_8$: C, 72.90; H, 3.82.; N, 7.09. Found: C, 73.00; H, 3.86; N, 7.07.

5,10-Bis(4-bromophenyl)-15,20-di(4-pyridyl)porphyrin (3). By use of a general method, 4-pyridinecarboxaldehyde (0.535g, 5 mmol), 4-bromobenzaldehyde (0.925g, 5 mmol), and 50 mL of propionic acid were added, and the reaction mixture was stirred under nitrogen. To increase the solubility of 4-bromobenzaldehyde, the reaction mixture was heated to 80 °C at which point the aldehyde was fully dissolved. Freshly distilled pyrrole (0.7 mL; 10 mmol) was then added to the mixture and allowed to stir for 4 h under reflux. Reaction mixture was brought to room temperature, and the reaction flask was then placed in the freezer overnight to aid precipitation of the porphyrin. The crude product was repeatedly chromatographed on silica gel. The purest compound was obtained by recrystallization in methanol. Yield: 3.87g (50%). Mp > 300 °C. ^{1}H NMR (500 MHz, $CDCl_3$ 298 K, δ [ppm]) −2.86 (s, 2H, NH), 7.94 (d, J = 7.5 Hz, 4H, Ph-Br), 8.10 (d, J = 7.5 Hz, 4H, Ph-Br), 8.18 (d, J = 10 Hz, 4H, pyridyl-H), 8.88 (m, 8H, β-H Py), 9.07 (d, J = 10 Hz, 4H, pyridyl-H). UV−vis (CH_2Cl_2, λ [nm], 298 K): 418 nm, 514 nm, 547 nm, 588 nm, 645 nm. MALDI-TOF MS (m/z): 775.399 (calcd for $C_{42}H_{26}Br_2N_6$ exact mass, 774.520). Anal. Calcd for $C_{42}H_{26}Br_2N_6$: C, 65.13; H, 3.38.; N, 10.85. Found: C, 65.14; H, 3.30; N, 10.72.

5,10-Bis(4-aminobiphenyl)-15,20-bis(4-pyridyl)porphyrin (4). A Schlenk tube was charged with 5,20-bis(4-bromophenyl)-10,15-di(pyridin-4-yl)porphyrin (0.054g, 0.07 mmol), 4-(4,4,5,5-tetramethyl-1,3,2-dioxaborolan-2-yl)aniline (0.092g, 0.42 mmol), K_3PO_4 (0.089g, 0.42 mmol), and $Pd(PPh_3)_4$ (8 mg, 0.007 mmol) under nitrogen atmosphere. Dioxane (5 mL) and deionized water (0.1 mL) were added, and the resulting mixture was refluxed for 24 h, brought to room temperature, and filtered through Celite in a sintered funnel. It was washed several times with DCM, and the filtrate was evaporated in vacuum. The crude product obtained upon evaporation of solvent was

DOI: 10.1021/acs.jmedchem.7b01297
J. Med. Chem. 2018, 61, 804−817

purified by silica gel column chromatography (100−200 mesh) using ethyl acetate/dichloromethane (20:80, v/v) as an eluent. Yield 44.6 mg (80%). Mp > 300 °C. ^{1}H NMR (500 MHz, $CDCl_3$ 298 K, δ [ppm]) −2.76 (s, 2H, NH), 3.75 (s, 4H, NH_2), 6.88(d, 2H, J = 8.5 Hz, β-H Py), 7.72 (d, 2H, J = 8.5 Hz, β-H Py), 7.91 (d, 4H, J = 7.5 Hz, Ph-H), 8.17 (d, 4H, J = 5.5 Hz, pyridyl-H), 8.20 (d, 4H, J = 8 Hz, Ph-H), 8.81 (d, 4H, J = 4 Hz, Ph-H), 8.84 (s, 2H, β-H Py), 8.97 (s, 2H, β-H Py), 9.01 (d, 4H, J = 4.5 Hz, Ph-H), 9.03 (d, 4H, J = 5 Hz, pyridyl-H). UV−vis (CH_2Cl_2, λ [nm], 298 K): 420 nm, 515 nm, 553 nm, 592 nm, 645 nm.MALDI-TOF MS (m/z): 798.820 (calcd for $C_{54}H_{38}N_8$ exact mass, 798.322). Anal. Calcd for $C_{54}H_{38}N_8$: C, 81.18; H, 4.79.; N, 14.03. Found: C, 81.14; H, 4.16; N, 14.12.

5,15-Bis(4-bromophenyl)-10,20-di(4-pyridyl)porphyrin (5). By use of a general method, 2,2′-((4-bromophenyl)methylene)bis-(1*H*-pyrrole) (0.5 g, 1.66 mmol) and 4-pyridinecarboxaldehyde (0.171g, 1.6 mmol) were taken in a round-bottom flask, and 40 mL of propionic acid was added to it. The reaction mixture was then stirred under nitrogen at 298 K for 90 min. Thereafter, the reaction mixture was refluxed under nitrogen for 90 min, brought to room temperature, and left overnight for precipitation at room temperature. The precipitate was poured into sintered funnel and washed several times with methanol. The crude product thus obtained was vacuum-dried followed by repeated silica gel column chromatography. The purest compound was obtained by recrystallization from methanol. Yield 620 mg (50%). Mp > 300 °C. ^{1}H NMR (500 MHz, $CDCl_3$ 298 K, δ [ppm]) −2.85 (s, 2H, NH), 7.9 (d, J = 8 Hz, 4H, Ph-Br), 8.10 (d, J = 7.5 Hz, 4H, Ph-Br), 8.18 (d, J = 5.5 Hz, 4H, pyridyl-H), 8.85 (br, 4H, β-H Py), 8.90 (br, 4H, β-H Py), 9.07 (d, J = 5 Hz, 4H, pyridyl-H). UV−vis (CH_2Cl_2, λ [nm], 298 K): 417 nm, 513 nm, 548 nm, 590 nm, 644 nm. MALDI-TOF MS (m/z): 772.425 (calcd for $C_{42}H_{26}Br_2N_6$ exact mass, 772.059).Anal. Calcd for for $C_{42}H_{26}Br_2N_6$: C, 65.13; H, 3.38.; N, 10.85. Found: C, 65.24; H, 3.40; N, 10.72.

5,15-Bis(4-bromophenyl)-10,20-bis(4-phenylpyridyl)-porphyrin (6). By use of a general method, 2,2′-((4 bromophenyl)-methylene)bis(1*H*-pyrrole) (0.5 g, 1.66 mmol) and 4-(pyridin-4-yl)benzaldehyde (0.304g, 1.6 mmol) were taken in a round-bottom flask and 40 mL of propionic acid was added. The reaction mixture was then stirred under nitrogen at 298 K for 90 min. Thereafter, the reaction mixture was refluxed under nitrogen for 90 min, brought to room temperature, and left overnight for precipitation. The precipitate was poured into sintered funnel and washed with methanol. The crude product left on the sintered funnel was then dried in vacuum. The crude product was purified by silica gel column chromatography (100−200 mesh) using ethyl acetate/dichloromethane (10:90, v/v) as an eluent. Yield: 296 mg (20%). Mp > 300 °C. ^{1}H NMR (500 MHz, $CDCl_3$ 298 K, δ [ppm]) −2.81 (s, 2H, NH), 8.91 (br, 4H, pyridyl-H),8.87 (br, 2H, Py-βH), 8.85 (br, 4H, pyridyl-H), 8.34 (d, J = 7.5 Hz, 2H, Py-βH), 8.09 (m,8H, 4-bromo Ph, Ph), 8.05 (d, J = 7.5 Hz, 2H, Py-βH), 7.92 (m,8H, 4-bromo Ph, Ph), 7.86 (d, J = 5.5 Hz, 2H, Py-βH), UV−vis (CH_2Cl_2, λ [nm], 298 K): 418 nm, 514 nm, 550 nm, 592 nm, 647 nm. MALDI-TOF MS (m/z): 925.670 (calcd for $C_{54}H_{34}Br_2N_6$ exact mass, 924.121). Anal. Calcd for $C_{54}H_{34}Br_2N_6$: C, 69.99; H, 3.70.; N, 9.07. Found: C, 69.94; H, 3.64; N, 9.02.

5-(4-Bromophenyl)-10,15,20-tri(4-pyridyl)porphyrin (7). By use of a general method, 4-pyridinecarboxaldehyde (1.605g, 15 mmol), 4-bromobenzaldehyde (0.925g, 5 mmol), and 50 mL of propionic acid were added and the reaction mixture was magnetically stirred. Freshly distilled pyrrole (1.4 mL; 20 mmol) was then added to the mixture, the temperature then brought to reflux and allowed to stir for 4 h at reflux. After allowing the reaction mixture to cool to room temperature, the reaction flask was placed in the freezer overnight to aid precipitation of the porphyrin. The reaction mixture was then vacuum filtered using a sintered funnel, and a dark purple solid was collected, washed with 5 × 50 mL of DCM, washed with methanol, and dried overnight. The solid was purified by silica gel column chromatography. Yield 2.08 g (15%). Mp > 300 °C. ^{1}H NMR (500 MHz, $CDCl_3$ 298 K, δ [ppm]) 9.06 (d, J = 5 Hz, 6H, pyridyl-H), 8.90 (d, J = 4.5 Hz, 2H, β-H Py), 8.86 (s, 4H, β-H Py), 8.83 (d, J = 4.5 Hz, 2H, β-H Py), 8.17 (d, J = 5 Hz, 6H, pyridyl-H), 8.07 (d, J = 8 Hz, 2H, phenyl- H), 7.92 (d, J = 8 Hz, 2H, phenyl-H). UV−vis (CH_2Cl_2, λ [nm], 298 K): 416 nm, 512 nm, 547 nm, 588 nm, 643 nm. MALDI-TOF MS (m/z): 696.658 (calcd for $C_{41}H_{26}BrN_7$ exact mass, 696.612). Anal. Calcd for $C_{41}H_{26}BrN_7$: C, 70.69; H, 3.76.; N, 14.08. Found: C, 69.70; H, 3.86; N, 14.19.

5,10-Bis(4-carboxyphenyl)-15,20-bis(4-dimethyl-aminophenyl)porphyrin (8). By use of a general method, 4-(dimethylamino)benzaldehyde (0.745g, 5 mmol), 4-formylbenzoic acid (0.75g, 5 mmol), and 50 mL of propionic acid were added and the reaction mixture was stirred under nitrogen. To increase the solubility of 4-formylbenzoic acid, the reaction mixture was heated to 80 °C at which point the aldehyde fully dissolved. Freshly distilled pyrrole (0.7 mL; 10 mmol) was then added to the reaction mixture and allowed to stir for 4 h under reflux. After allowing the reaction mixture to cool to room temperature, the reaction flask was placed in the freezer overnight to aid precipitation of the porphyrin. The precipitate was vacuum filtered through a sintered funnel, and a dark purple solid so collected was washed with methanol and dried. The solid residue was purified over silica gel chromatography and recrystallized from methanol. Yield: 1.57g (20%). Mp > 300 °C. ^{1}H NMR (500 MHz, DMSO-d_6 298 K, δ [ppm]) 12.85 (2H, br, -COOH), 8.96 (br, 4H, carboxyPh-CH), 8.82 (br, 6H, carboxyPh-CH and Py-β-CH), 8.38 (d, J = 7.5 Hz, 4H, *N*,*N*-dimethyl Ph), 8.33 (d, J = 7.5 Hz, 4H, *N*,*N*-dimethyl Ph), 8.03 (d, J = 7.5 Hz, 2H, Py-β-CH),7.95 (s, 2H, Py-β-CH), 7.16 (d, J = 8 Hz, 2H, Py-β-CH), 2.89 (s, 12H, Me), −2.84 (br, 2H, NH). UV−vis (CH_2Cl_2, λ [nm], 298 K): 414 nm, 516 nm, 557 nm, 594 nm, 652 nm. MALDI-TOF MS (m/z): 788.681 (calcd for $C_{50}H_{40}N_6O_4$ exact mass, 788.311). Anal. Calcd for $C_{50}H_{40}N_6O_4$: C, 76.12; H, 5.11.; N, 10.65. Found: C, 76.14; H, 5.16; N, 10.62.

5-(4-Carboxyphenyl)-10,15,20-tri(4-dimethylaminophenyl)-porphyrin (9). By use of a general method, 4-(dimethylamino)-benzaldehyde (2.23g, 15 mmol) and 4-formylbenzoic acid (0.75g, 5 mmol) were added to 50 mL of propionic acid, and the reaction mixture was magnetically stirred. Freshly distilled pyrrole (1.4 mL; 20 mmol) was then added to the mixture, the temperature then brought to reflux and allowed to stir for 4 h at reflux. After allowing the reaction mixture to cool to room temperature, the reaction flask was placed in the freezer overnight to aid precipitation of the porphyrin. The reaction mixture was then vacuum filtered using a sintered funnel, and a dark purple solid was collected, washed with 5 × 50 mL of DCM, washed with methanol, and dried overnight. The solid residue was purified over silica gel chromatography using 30% EtOAc−CH_2Cl_2. Yield 3.1 g (20%). Mp > 300 °C. ^{1}H NMR (500 MHz, $CDCl_3$ 298 K, δ [ppm]) 12.85 (1H, br, -COOH),8.92 (br, 2H, carboxyPh-CH), 8.75 (br, 2H, carboxyPh-CH), 8.57 (s, 4H, Py-β-CH), 8.42 (br, 6H, *N*,*N*-dimethyl Ph), 8.28 (br, 6H, *N*,*N*-dimethyl Ph), 8.06 (d, J = 7 Hz, 2H, Py-β-CH), 7.10 (d, J = 7 Hz, 2H, Py-β-CH), 3.32 (s, 18H, Me), −2.70 (br, 2H, NH). UV−vis (CH_2Cl_2, λ [nm], 298 K): 417 nm, 519 nm, 561 nm, 598 nm, 655 nm. MALDI-TOF MS (m/z): 787.918 (calcd for $C_{51}H_{45}N_7O_2$ exact mass, 787.363). Anal. Calcd for $C_{51}H_{45}N_7O_2$:C, 77.74; H, 5.76.; N, 12.44. Found: C, 77.80; H, 5.81; N, 12.41.

5,10,15,20-Tetra(4-pyridyl)porphyrin (10). By use of a general method, 1.07 g (10 mmol) of 4-pyridinecarboxaldehyde and 50 mL of propionic acid were added and the reaction mixture was magnetically stirred. Freshly distilled pyrrole (0.7 mL; 10 mmol) was then added to the mixture, the temperature then brought to reflux and allowed to stir for 2 h at reflux. After allowing the reaction mixture to cool to room temperature, the reaction flask was placed in the freezer overnight to aid precipitation of the porphyrin. The reaction mixture was then vacuum filtered using a sintered funnel, and a dark purple solid was collected, washed with 5 × 50 mL of DCM, washed with methanol, and dried overnight to give 5,10,15,20-tetra(4-pyridyl)porphyrin.Yield 2.472 g (20%). Mp > 300 °C. ^{1}H NMR (500 MHz, $CDCl_3$ 298 K, δ [ppm]) 8.94 (d, J = 5 Hz, 8H, pyridyl-H), 8.79(b, 8H, pyrrole β-H), 8.16 (d, J = 5 Hz, 8H, pyridyl- H), −2.99 (b, 2H, pyrrole NH). UV−vis (CH_2Cl_2, λ [nm], 298 K): 415 nm, 511 nm, 545 nm, 587 nm, 642 nm. MALDI-TOF MS (m/z): 618.629 (calcd for $C_{40}H_{26}N_8$ exact mass, 618.704). Anal. Calcd for $C_{40}H_{26}N_8$: C, 77.65; H, 4.24.; N, 18.11. Found: C, 77.00; H, 4.16; N, 18.07.

DOI: 10.1021/acs.jmedchem.7b01297
J. Med. Chem. 2018, 61, 804−817

Drug and Antibodies. Camptothecin, proteasomal inhibitor MG132, and *N*-acetyl-L-cysteine (NAC) were purchased from Sigma. Mouse monoclonal anti-human Top1 (C21) antibody, rabbit polyclonal PARP1 antibody, and secondary antibodies horseradish peroxidase conjugated anti-rabbit IgG and anti-mouse IgG were obtained from Santa Cruz Biotechnology (USA). Anti-actin (ACTN05) antibody was from Neo Markers (USA).

Recombinant Human Topoisomerase 1 and Plasmid DNA Relaxation Assay. The recombinant human Top1 was purified from Sf-9 insect cells, infected with the recombinant baculovirus (a kind gift from Prof. James. J. Champoux) as described previously.[6,13]

The type 1 DNA topoisomerase is assayed by decreased mobility of the relaxed isomers of supercoiled pBS (SK^+) DNA in 1% agarose gel. The relaxation assay was carried out with recombinant human Top1 or the whole cell extracts of human breast adenocarcinoma (MCF7) cells as source of endogenous Top1, diluted in the relaxation buffer with supercoiled plasmid DNA as described previously.[6,8,13,38]

Cleavage Assay. Plasmid DNA cleavage assay was carried out as described previously.[6,8] For equilibrium cleavage assays, 25-mer duplex of oligonucleotide containing a Top1 binding motif was labeled and annealed as described previously.[13,36,38] Samples were analyzed by 12% sequencing gel electrophoresis, dried, and exposed on PhosphorImager screens and imaged with Typhoon FLA 7000 (GE Healthcare, U.K.).

Cell Culture and Transfection. Human cancerous cell lines like MCF7, HeLa, HCT116, NIH:OVCAR-3, and HEK293 were obtained from the Developmental Therapeutics Program as kind gift from Dr. Yves Pommier (NIH/NCI/USA). $TDP1^{+/+}$ and $TDP1^{-/-}$ primary MEF cells were kind gift from Dr. Cornelius F. Boerkoel (University of British Columbia, Canada) and were cultured as described previously.[6,36,40,42] Plasmid DNAs were transfected with Lipofectamine 2000 (Invitrogen) according to the manufacturer's protocol.

Photobleaching Experiments. Photobleaching experiments were performed as described formerly[40−42] using Andor Spining disk inverted confocal laser-scanning microscope equipped with a 60×/1.42 NA oil-immersion objective (Olympus) and with a CO_2-controlled on-stage heated environmental chamber set to 37 °C. FRAP analyses were carried out with living MCF7 cells ectopically expressing EGFP-human Top1 grown on chamber cover glass (Genetix, India) and drug treated as indicated. For FRAP analysis, a subnuclear spot was bleached for 30 ms by solid-state laser line (488 nm for EGFP) adapted to the fluorescent protein of interest and FRAP curves were generated individually normalized to the prebleach signal as described previously.[42]

Job Plot and Spectrofluorimetric Binding Assay. The binding stoichiometry for compound **8** with Top1 was determined using the method of continuous variation.[12,14,43] Briefly, reaction mixtures containing variable Top1 and compound **8** to a final concentration of 1.25 μM were analyzed for quenching of tryptophan fluorescence at 350 nm upon excitation at 295 nm on PerkinElmer LS55 luminescence spectrometer.

Spectrofluorimetric binding assay was carried out as previously described[12,14,43] where Top1 (200 nM) was incubated with various concentrations of compound **8** (0−11 μM) at 25 °C for 10 min. The equation for determining fraction of binding sites (B) occupied by inhibitor was $B = (F_0 - F)/F_{max}$, where F_0 is the fluorescence intensity at 350 nm of Top1 alone in the absence of any inhibitors, F is the fluorescence intensity at 350 nm of Top1 in the presence of inhibitor, and F_{max} is obtained from the plot of $1/(F_0 - F)$ versus 1/[X] and by extrapolating 1/[X] to zero, where [X] is the concentration of compound **8**. The dissociation constant (K_D) was determined as described previously.[12]

Analysis of Compound 8-DNA Intercalation. The competence of the drug to intercalate into plasmid DNA was determined by Top1 unwinding assay.[36,44] Assays were performed with 50 fmol of pBluscript (SK+) DNA in the presence or absence of compound **8**, m-AMSA, and etoposide at indicated concentrations. Excess of DNA topoisomerase I was reacted with supercoiled plasmid DNA to generate relaxed DNA for the unwinding assays. The relaxed DNA was purified by proteolytic digestion with proteinase K at 37 °C, followed by phenol/chloroform extraction and ethanol precipitation. The unwinding assays were carried out at 37 °C for 15 min with independent compounds and were analyzed by 1% agarose gel as described above.

Cell Extracts and Immunoblotting. Preparation of whole cell extracts from MCF7 cells and immunoblotting were carried out as described.[6,40,41] Immunoreactivity was detected using ECL chemiluminescence reaction (Amersham) under ChemiDoc MP system (Bio-Rad, USA).

Immuno Complex of Enzyme (ICE) Bioassay. In vivo Top1 cleavage complexes (Top1cc) were isolated from MCF7 cells using immuno complex of enzyme (ICE) bioassay technique.[49] Briefly, 5×10^6 MCF7 cells were treated with drugs and were lysed by DNAzol reagent (Invitrogen, USA) in the presence of 0.1% SDS. Genomic DNA was prepared and was briefly sonicated. Varying concentrations of DNA were spotted onto nitrocellulose membrane (Millipore, USA) using a slot-blot vacuum system (Biorad, USA). Immunoblotting was carried out with antihuman Top1 antibodies as described.[41]

Measurement of ROS. Intracellular ROS was detected in drug-treated MCF7 cells with or without pretreatment of *N*-acetyl-L-cysteine (NAC) for indicated time as described.[13,46] Briefly, cells were washed and resuspended in 500 μL of 1× PBS and were loaded with 2 μg/mL of H_2DCFDA (Molecular Probes) for 30 min, and green fluorescence of 2,7-dichlorofluorescein was measured at 515 nm by spectrofluorometer.

Alkaline COMET Assays. To detect the levels of drug-induced DNA breaks, after treatment MCF7 cells were subjected to alkaline comet assays according to the manufacturer's instructions (Trevigen, USA) and comet length was measured and was scored for at least 50 cells. Distributions of comet lengths were compared using the Student's *t*-test as described previously.[13,40,50]

Immunocytochemistry. Immunofluorescence staining of apoptosis marker phosphatidylserine was performed as described previously.[40,41] After treatment, MCF7 cells were fixed with 2% paraformaldehyde for 10 min at room temperature and stained with annexin V-FITC antibody (BD, USA), mounted in antifade solution with propidium iodide (Vector Laboratories, USA), and examined under Leica TCS SP8 confocal laser-scanning microscope.

Cell Survival Assay. Cell survival was assessed by 3-(4,5-dimethylthiazol-2-yl)-2,5-diphenyltetrazolium bromide (MTT) assay as discussed previously.[6] The percent inhibition of viability for each concentration of the compounds was calculated with respect to the control, and IC_{50} values were estimated.

siRNA Transfection. Transfections were performed as described previously.[40] In brief, cells (1.5×10^5) were transfected with control siRNA or 40 nM Top1 siRNA (Qiagen) using oligofectamine (Invitrogen) according to the manufacturer's protocol. Time course experiments revealed a maximum suppression of Top1 protein at day 3 after transfection, as analyzed by Western blotting.

■ ASSOCIATED CONTENT

Supporting Information

The Supporting Information is available free of charge on the ACS Publications website at DOI: 10.1021/acs.jmedchem.7b01297.

MALDI-TOF MS, ^{1}H NMR, and ^{1}H−^{1}H 2D COSY spectra and UV−vis data of compounds **1**−**10** (PDF)

Molecular formula strings (CSV)

■ AUTHOR INFORMATION

Corresponding Authors

*H.R.: e-mail, ichr@iacs.res.in.

*B.B.D.: phone, +91 33 2473 4971, extension 2108; fax, +91 33 2473 2805; e-mail, pcbbd@iacs.res.in.

ORCID

Harapriya Rath: 0000-0002-5507-5275

Benu Brata Das: 0000-0003-2519-7105

DOI: 10.1021/acs.jmedchem.7b01297
J. Med. Chem. 2018, 61, 804−817

Notes

The authors declare no competing financial interest.

■ ACKNOWLEDGMENTS

We thank Dr. Hemanta K Majumder and Dr. Suvendra N Bhattacharyya, CSIR-Indian Institute of Chemical Biology, India for their help during the study and Mr. Gopal K Manna of IACS for his help with the artwork. The BBD team is supported by Wellcome Trust/DBT India Alliance Intermediate Fellowship (Award IA/I/13/1/500888) and also funded the open access charge. A.G. and K.C.S. are recipients of CSIR-NET-Senior Research Fellowship, India. S.P.C. thanks UGC-CSIR-NET for Junior Research Fellowship. S.K.D., I.R., and N.H. thank IACS for SRF and JRF positions, respectively. H.R. thanks DST-SERB (Grant EMR/2016/004705) for the research grant. B.B.D. is a Wellcome Trust/DBT India Alliance Intermediate Fellow.

■ REFERENCES

(1) Champoux, J. J. DNA topoisomerases: structure, function, and mechanism. *Annu. Rev. Biochem.* **2001**, *70*, 369−413.
(2) Capranico, G.; Marinello, J.; Chillemi, G. Type I DNA topoisomerases. *J. Med. Chem.* **2017**, *60*, 2169−2192.
(3) Pommier, Y. Drugging topoisomerases: lessons and challenges. *ACS Chem. Biol.* **2013**, *8*, 82−95.
(4) Pommier, Y. DNA topoisomerase I inhibitors: chemistry, biology, and interfacial inhibition. *Chem. Rev.* **2009**, *109*, 2894−2902.
(5) Pommier, Y. Topoisomerase I inhibitors: camptothecins and beyond. *Nat. Rev. Cancer* **2006**, *6*, 789−802.
(6) Majumdar, P.; Bathula, C.; Basu, S. M.; Das, S. K.; Agarwal, R.; Hati, S.; Singh, A.; Sen, S.; Das, B. B. Design, synthesis and evaluation of thiohydantoin derivatives as potent topoisomerase I (top1) inhibitors with anticancer activity. *Eur. J. Med. Chem.* **2015**, *102*, 540−551.
(7) Nagarajan, M.; Morrell, A.; Antony, S.; Kohlhagen, G.; Agama, K.; Pommier, Y.; Ragazzon, P. A.; Garbett, N. C.; Chaires, J. B.; Hollingshead, M.; Cushman, M. Synthesis and biological evaluation of bisindenoisoquinolines as topoisomerase I inhibitors. *J. Med. Chem.* **2006**, *49*, 5129−5140.
(8) Cushman, M.; Jayaraman, M.; Vroman, J. A.; Fukunaga, A. K.; Fox, B. M.; Kohlhagen, G.; Strumberg, D.; Pommier, Y. Synthesis of new indeno[1,2-c]isoquinolines: cytotoxic non-camptothecin topoisomerase I inhibitors. *J. Med. Chem.* **2000**, *43*, 3688−3698.
(9) Pommier, Y.; Sun, Y.; Huang, S. N.; Nitiss, J. L. Roles of eukaryotic topoisomerases in transcription, replication and genomic stability. *Nat. Rev. Mol. Cell Biol.* **2016**, *17*, 703−721.
(10) Wu, N.; Wu, X. W.; Agama, K.; Pommier, Y.; Du, J.; Li, D.; Gu, L. Q.; Huang, Z. S.; An, L. K. A novel DNA topoisomerase I inhibitor with different mechanism from camptothecin induces G2/M phase cell cycle arrest to K562 cells. *Biochemistry* **2010**, *49*, 10131−10136.
(11) Yu, L. M.; Zhang, X. R.; Li, X. B.; Yang, Y.; Wei, H. Y.; He, X. X.; Gu, L. Q.; Huang, Z. S.; Pommier, Y.; An, L. K. Synthesis and biological evaluation of 6-substituted indolizinoquinolinediones as catalytic DNA topoisomerase I inhibitors. *Eur. J. Med. Chem.* **2015**, *101*, 525−533.
(12) Chowdhury, S.; Mukherjee, T.; Sengupta, S.; Chowdhury, S. R.; Mukhopadhyay, S.; Majumder, H. K. Novel betulin derivatives as antileishmanial agents with mode of action targeting type IB DNA topoisomerase. *Mol. Pharmacol.* **2011**, *80*, 694−703.
(13) Ganguly, A.; Das, B.; Roy, A.; Sen, N.; Dasgupta, S. B.; Mukhopadhayay, S.; Majumder, H. K. Betulinic acid, a catalytic inhibitor of topoisomerase I, inhibits reactive oxygen species-mediated apoptotic topoisomerase I-DNA cleavable complex formation in prostate cancer cells but does not affect the process of cell death. *Cancer Res.* **2007**, *67*, 11848−11858.
(14) Saha, S.; Acharya, C.; Pal, U.; Chowdhury, S. R.; Sarkar, K.; Maiti, N. C.; Jaisankar, P.; Majumder, H. K. A novel spirooxindole derivative inhibits the growth of Leishmania donovani parasites both in vitro and in vivo by targeting type IB topoisomerase. *Antimicrob. Agents Chemother.* **2016**, *60*, 6281−6293.
(15) Sordet, O.; Khan, Q. A.; Plo, I.; Pourquier, P.; Urasaki, Y.; Yoshida, A.; Antony, S.; Kohlhagen, G.; Solary, E.; Saparbaev, M.; Laval, J.; Pommier, Y. Apoptotic topoisomerase I-DNA complexes induced by staurosporine-mediated oxygen radicals. *J. Biol. Chem.* **2004**, *279*, 50499−50504.
(16) Sordet, O.; Goldman, A.; Pommier, Y. Topoisomerase II and tubulin inhibitors both induce the formation of apoptotic topoisomerase I cleavage complexes. *Mol. Cancer Ther.* **2006**, *5*, 3139−3144.
(17) Sen, N.; Banerjee, B.; Das, B. B.; Ganguly, A.; Sen, T.; Pramanik, S.; Mukhopadhyay, S.; Majumder, H. K. Apoptosis is induced in leishmanial cells by a novel protein kinase inhibitor withaferin A and is facilitated by apoptotic topoisomerase I-DNA complex. *Cell Death Differ.* **2007**, *14*, 358−367.
(18) Sordet, O.; Goldman, A.; Redon, C.; Solier, S.; Rao, V. A.; Pommier, Y. Topoisomerase I requirement for death receptor-induced apoptotic nuclear fission. *J. Biol. Chem.* **2008**, *283*, 23200−23208.
(19) Teo, R. D.; Hwang, J. Y.; Termini, J.; Gross, Z.; Gray, H. B. Fighting cancer with corroles. *Chem. Rev.* **2017**, *117*, 2711−2729.
(20) Zou, Q.; Abbas, M.; Zhao, L.; Li, S.; Shen, G.; Yan, X. Biological photothermal nanodots based on self-assembly of peptide-porphyrin conjugates for antitumor therapy. *J. Am. Chem. Soc.* **2017**, *139*, 1921−1927.
(21) Karunakaran, S. C.; Ramaiah, D.; Schulz, I.; Epe, B. Study of the mode and efficiency of DNA binding in the damage induced by photoactivated water soluble porphyrins. *Photochem. Photobiol.* **2013**, *89*, 1100−1105.
(22) Munson, B. R.; Fiel, R. J. DNA intercalation and photosensitization by cationic meso substituted porphyrins. *Nucleic Acids Res.* **1992**, *20*, 1315−1319.
(23) Shuai, L.; Wang, S.; Zhang, L.; Fu, B.; Zhou, X. Cationic porphyrins and analogues as new DNA topoisomerase I and II inhibitors. *Chem. Biodiversity* **2009**, *6*, 827−837.
(24) Zhai, B.; Shuai, L.; Yang, L.; Weng, X.; Wu, L.; Wang, S.; Tian, T.; Wu, X.; Zhou, X.; Zheng, C. Octa-substituted anionic porphyrins: topoisomerase I inhibition and tumor cell apoptosis induction. *Bioconjugate Chem.* **2008**, *19*, 1535−1542.
(25) Adler, A. D.; Longo, F. R.; Finarelli, J. D.; Goldmacher, J.; Assour, J.; Korsakoff, L. A simplified synthesis for meso-tetraphenylporphine. *J. Org. Chem.* **1967**, *32*, 476−476.
(26) Harada, A.; Yamaguchi, H.; Okamoto, K.; Fukushima, H.; Shiotsuki, K.; Kamachi, M. Control of photoinduced electron transfer from zinc-porphyrin to methyl viologen by supramolecular formation between monoclonal antibody and zinc-porphyrin. *Photochem. Photobiol.* **1999**, *70*, 298−302.
(27) Fouad, F. S.; Crasto, C. F.; Lin, Y.; Jones, G. B. Photoactivated enediynes: targeted chimeras which undergo photo-bergman cyclization. *Tetrahedron Lett.* **2004**, *45*, 7753−7756.
(28) Ikeda, T.; Shinkai, S.; Sada, K.; Takeuchi, M. A preliminary step toward molecular spring driven by cooperative guest binding. *Tetrahedron Lett.* **2009**, *50*, 2006−2009.
(29) Smith, M. W.; Lawton, L. G.; Checkoff, J. Tetrapyridyl porphyrin derivatives of group 13 metals. *Synth. React. Inorg. Met.-Org. Chem.* **1993**, *23*, 639−651.
(30) Adler, A. D.; Sklar, L.; Longo, F. R.; Finarelli, J. D.; Finarelli, M. G. A mechanistic study of the synthesis of meso-tetraphenylporphin. *J. Heterocycl. Chem.* **1968**, *5*, 669−678.
(31) Zhang, X.-X.; Wayland, B. B. Rhodium(II) porphyrin bimetalloradical complexes: preparation and enhanced reactivity with CH4 and H2. *J. Am. Chem. Soc.* **1994**, *116*, 7897−7898.
(32) DiMagno, S. G.; Lin, V. S. Y.; Therien, M. J. Catalytic conversion of simple haloporphyrins into alkyl-, aryl-, pyridyl-, and vinyl-substituted porphyrins. *J. Am. Chem. Soc.* **1993**, *115*, 2513−2515.
(33) Hyslop, A. G.; Therien, M. J. Synthesis of porphyrin-spacer-quinone compounds via metal-mediated cross-coupling: new systems for probing the relative magnitudes of axial and equatorial electronic

DOI: 10.1021/acs.jmedchem.7b01297
J. Med. Chem. 2018, 61, 804−817

coupling at the porphyrin macrocycle in thermal and photoactivated electron transfer reactions. *Inorg. Chim. Acta* **1998**, *275*, 427−434.
(34) Nowak-Król, A.; Koszarna, B.; Yoo, S. Y.; Chromiński, J.; Węcławski, M. K.; Lee, C.-H.; Gryko, D. T. Synthesis of trans-A2B2-porphyrins bearing phenylethynyl substituents. *J. Org. Chem.* **2011**, *76*, 2627−2634.
(35) Ravikanth, M.; Strachan, J.-P.; Li, F.; Lindsey, J. S. Trans-substituted porphyrin building blocks bearing iodo and ethynyl groups for applications in bioorganic and materials chemistry. *Tetrahedron* **1998**, *54*, 7721−7734.
(36) Das, B. B.; Sen, N.; Roy, A.; Dasgupta, S. B.; Ganguly, A.; Mohanta, B. C.; Dinda, B.; Majumder, H. K. Differential induction of Leishmania donovani bi-subunit topoisomerase I-DNA cleavage complex by selected flavones and camptothecin: activity of flavones against camptothecin-resistant topoisomerase I. *Nucleic Acids Res.* **2006**, *34*, 1121−1132.
(37) Gentry, A. C.; Juul, S.; Veigaard, C.; Knudsen, B. R.; Osheroff, N. The geometry of DNA supercoils modulates the DNA cleavage activity of human topoisomerase I. *Nucleic Acids Res.* **2011**, *39*, 1014−1022.
(38) Das, B. B.; Sen, N.; Dasgupta, S. B.; Ganguly, A.; Majumder, H. K. N-terminal region of the large subunit of Leishmania donovani bisubunit topoisomerase I is involved in DNA relaxation and interaction with the smaller subunit. *J. Biol. Chem.* **2005**, *280*, 16335−16344.
(39) Marchand, C.; Huang, S. Y.; Dexheimer, T. S.; Lea, W. A.; Mott, B. T.; Chergui, A.; Naumova, A.; Stephen, A. G.; Rosenthal, A. S.; Rai, G.; Murai, J.; Gao, R.; Maloney, D. J.; Jadhav, A.; Jorgensen, W. L.; Simeonov, A.; Pommier, Y. Biochemical assays for the discovery of TDP1 inhibitors. *Mol. Cancer Ther.* **2014**, *13*, 2116−2126.
(40) Das, B. B.; Antony, S.; Gupta, S.; Dexheimer, T. S.; Redon, C. E.; Garfield, S.; Shiloh, Y.; Pommier, Y. Optimal function of the DNA repair enzyme TDP1 requires its phosphorylation by ATM and/or DNA-PK. *EMBO J.* **2009**, *28*, 3667−3680.
(41) Das, B. B.; Huang, S. Y.; Murai, J.; Rehman, I.; Ame, J. C.; Sengupta, S.; Das, S. K.; Majumdar, P.; Zhang, H.; Biard, D.; Majumder, H. K.; Schreiber, V.; Pommier, Y. PARP1-TDP1 coupling for the repair of topoisomerase I-induced DNA damage. *Nucleic Acids Res.* **2014**, *42*, 4435−4449.
(42) Das, S. K.; Rehman, I.; Ghosh, A.; Sengupta, S.; Majumdar, P.; Jana, B.; Das, B. B. Poly(ADP-ribose) polymers regulate DNA topoisomerase I (Top1) nuclear dynamics and camptothecin sensitivity in living cells. *Nucleic Acids Res.* **2016**, *44*, 8363−8375.
(43) Huang, C. Y. Determination of binding stoichiometry by the continuous variation method: the Job plot. *Methods Enzymol.* **1982**, *87*, 509−525.
(44) Chen, G. L.; Yang, L.; Rowe, T. C.; Halligan, B. D.; Tewey, K. M.; Liu, L. F. Nonintercalative antitumor drugs interfere with the breakage-reunion reaction of mammalian DNA topoisomerase II. *J. Biol. Chem.* **1984**, *259*, 13560−13566.
(45) Pommier, Y.; Huang, S. Y.; Gao, R.; Das, B. B.; Murai, J.; Marchand, C. Tyrosyl-DNA-phosphodiesterases (TDP1 and TDP2). *DNA Repair* **2014**, *19*, 114−129.
(46) Sen, N.; Das, B. B.; Ganguly, A.; Mukherjee, T.; Tripathi, G.; Bandyopadhyay, S.; Rakshit, S.; Sen, T.; Majumder, H. K. Camptothecin induced mitochondrial dysfunction leading to programmed cell death in unicellular hemoflagellate Leishmania donovani. *Cell Death Differ.* **2004**, *11*, 924−936.
(47) Soldani, C.; Scovassi, A. I. Poly(ADP-ribose) polymerase-1 cleavage during apoptosis: an update. *Apoptosis* **2002**, *7*, 321−328.
(48) Hirano, R.; Interthal, H.; Huang, C.; Nakamura, T.; Deguchi, K.; Choi, K.; Bhattacharjee, M. B.; Arimura, K.; Umehara, F.; Izumo, S.; Northrop, J. L.; Salih, M. A.; Inoue, K.; Armstrong, D. L.; Champoux, J. J.; Takashima, H.; Boerkoel, C. F. Spinocerebellar ataxia with axonal neuropathy: consequence of a TDP1 recessive neomorphic mutation? *EMBO J.* **2007**, *26*, 4732−4743.
(49) Regairaz, M.; Zhang, Y. W.; Fu, H.; Agama, K. K.; Tata, N.; Agrawal, S.; Aladjem, M. I.; Pommier, Y. Mus81-mediated DNA cleavage resolves replication forks stalled by topoisomerase I-DNA complexes. *J. Cell Biol.* **2011**, *195*, 739−749.
(50) El-Khamisy, S. F.; Saifi, G. M.; Weinfeld, M.; Johansson, F.; Helleday, T.; Lupski, J. R.; Caldecott, K. W. Defective DNA single-strand break repair in spinocerebellar ataxia with axonal neuropathy-1. *Nature* **2005**, *434*, 108−113.

DOI: 10.1021/acs.jmedchem.7b01297
J. Med. Chem. 2018, 61, 804−817